

See discussions, stats, and author profiles for this publication at: <https://www.researchgate.net/publication/335590540>

Parametric modeling simulation for an origami shaped canopy

Article in *Frontiers of Architectural Research* · September 2019

DOI: 10.1016/j.foar.2019.08.001

CITATIONS

8

READS

4,157

2 authors:



Caio De Carvalho Lucarelli

Universidade Federal de Viçosa (UFV)

5 PUBLICATIONS 13 CITATIONS

[SEE PROFILE](#)



Joyce Carlo

Universidade Federal de Viçosa (UFV)

84 PUBLICATIONS 368 CITATIONS

[SEE PROFILE](#)

Some of the authors of this publication are also working on these related projects:



Building design with support of optimization methods [View project](#)



Bioclimatic techniques and technologies applied to building energy performance [View project](#)

Available online at www.sciencedirect.com

ScienceDirect

journal homepage: www.keaipublishing.com/foar

Research Article

Parametric modeling simulation for an origami shaped canopy

Caio D.C. Lucarelli*, Joyce C. Carlo

Department of Architecture and Urban Planning, Universidade Federal de Viçosa, Viçosa, 36570-000, Brazil

Received 1 March 2019; received in revised form 25 July 2019; accepted 5 August 2019

KEYWORDS

Parameterization;
Radiation analysis;
ASHRAE adaptive
comfort;
Statistical analysis;
Complex surfaces

Abstract This study perceives the developing process of a parameterization modeling in Grasshopper® for complex surfaces using building simulation, considering Annual Average of Hourly Radiation as the key-variable. The major goal of this article is to create, simulate and analyze through factorial analysis a modular canopy, based on Origami. The methodology applied consisted of the selection of the form, canopy parameterization, factorial analysis and simulation for radiation. Ladybug®, together with EnergyPlus™, were used to carry out the simulations. The object of study was the process of creation of a canopy. In countries with hot and humid climates, such as Brazil, the roofing areas are critical parts of building envelopes, highly susceptible to solar radiation. The simulation was performed for a full year for Viçosa, MG (Latitude 20° 45' 14" S, Longitude 42° 52' 55" W, Altitude 648 m), but due to parameterization, the canopy can be simulated anywhere else. As main results, the factorial analysis contributed for determining that the slope of the canopy was the most robust factor to the detriment of the cardinal and collateral orientations. For the best case scenario, the simulation generated levels of comfort of about 74.0% with 15.4% Hot and 10.6% Cold for natural conditioned spaces.

© 2019 Higher Education Press Limited Company. Production and hosting by Elsevier B.V. on behalf of KeAi. This is an open access article under the CC BY-NC-ND license (<http://creativecommons.org/licenses/by-nc-nd/4.0/>).

1. Introduction

The growing awareness of the impact of buildings on energy consumption and indirect carbon emissions is generating an interest among practitioners in developing projects that go

beyond energy compliance limits to maximize optimization. Instead of analyzing and choosing from a range of possible solutions, as shown by Sadineni et al. (2011), designers must predetermine the failure of the building design in the early stages to obtain fast and interactive feedback.

According to Delgarm et al. (2016), "energy is one of the most important resources used by the modern society and is the core of the economic and social activities in the industrialized countries" (Delgarm et al., 2016, pp. 293).

* Corresponding author.

E-mail address: caio.lucarelli@ufv.br (C.D.C. Lucarelli).

Peer review under responsibility of Southeast University.

<https://doi.org/10.1016/j.foar.2019.08.001>

2095-2635/© 2019 Higher Education Press Limited Company. Production and hosting by Elsevier B.V. on behalf of KeAi. This is an open access article under the CC BY-NC-ND license (<http://creativecommons.org/licenses/by-nc-nd/4.0/>).

Please cite this article as: Lucarelli, C.D.C., Carlo, J.C., Parametric modeling simulation for an origami shaped canopy, Frontiers of Architectural Research, <https://doi.org/10.1016/j.foar.2019.08.001>

Over the past 50 years, we have seen a large increase in global energy demand for industrial development and due to population growth. Therefore, improvements in energy efficiency have become an important international business, for both designers and researchers.

This article is circumscribed to the steps of developing a performance-based canopy inspired by Origami shapes. It takes into account the discussion on how the energy and other related simulation approaches are necessary for performance evaluation and parameterization of the form in the primary stages of design. The first aspects considered were the form of the object and solar radiation. Considering design aspects, such as scaling in *X* axes, scaling in *Y* axes and deviation, as optimization parameters, it is possible to modify the surface of the canopy in order to achieve the objective of reducing beam radiation, and maximizing diffuse radiation. The optimization parameters are selected through the use of statistical analysis.

This paper aims to evaluate the process of creation of a modular canopy based on Origami shapes and complex surfaces, capable of allowing the entry of radiation indoors, thus maximizing diffuse incident radiation per square meter and minimizing beam radiation, according to solar geometry, through computer simulation, radiation optimization and statistical analysis.

2. Literature review

2.1. Energy consumption and daylighting

"Considering the importance of buildings in the total energy consumption and the fact that the constructive envelopes are responsible for the thermal exchanges with the [external] environment, as well as the admission of daylight" (Cartana et al., 2018, pp. 1684, our translation), the energy performance of wrapping systems has become increasingly important in contemporary architectural production, according to Fajkus (2013). In this scenario, shading strategies can contribute positively to the performance of buildings.

According to Sadineni et al. (2011), "a significant portion of the energy is consumed by today's buildings" (Sadineni et al., 2011, pp. 3618). This highlights the imperative need for energy savings. Therefore, shading devices can contribute to improve building performance.

Regarding thermal issues, Cho et al. (2014), evaluated the application of shading devices and identified that the radiated heat gains in general office buildings in South Korea accounted for about 33%–40% of the energy consumed by the construction sector from May to September, with annual maximum cooling load reduction of 19.7%. According to the International Energy Agency (IEA, 2010), the same buildings currently account for 40% of the energy consumption in most countries. A significant part of it is used for heating and cooling systems to bring comfort to the users of the buildings. In addition, Bader and Zitzler (2011) state that beam radiation may be reduced in the order of 75%, considering the use of the mentioned control elements, with good visual access to outdoors.

Sadineni et al. (2011) provide an exhaustive technical review of the building envelope components for the potential of their passive energy savings. They state that roofs are critical parts of the building envelope and are highly susceptible to solar radiation and other environmental changes, which affects indoor comfort conditions. Canopies account for substantial heat gain/loss, notably in countries near the Ecuador Line, including Brazil, despite the fact that they are usually left aside.

Jakubiec and Reinhart (2011) observed that solar shading elements can also improve the distribution of natural light and reduce the likelihood of visual discomfort. According to Reinhart and Wienold (2011), an integrated assessment of the luminous performance of a building should consider the annual availability of natural light, visual comfort and thermal loads in the form of radiation analysis. "Daylighting design hence becomes a tradeoff between optimizing the annual daylight availability within a space while making sure that the space is energy efficient and exhibits high occupant satisfaction." (Reinhart and Wienold, 2011, pp. 387).

2.2. Computational design process

According to Brotas and Rusovan (2013), architects rely much on computational tools to investigate forms and structures. Likewise, these tools cannot be used only for shape generation, but also to predict the performance of spaces.

As stated by González and Fiorito (2015), the integration of daylight and energy performance with the design simulation process has always been a challenge for designers. Most environmental performance simulation tools require a considerable amount of time and interactions to obtain accurate results. "Moreover the combination of daylight and energy performance has always been an issue, as different software packages are needed to perform detailed calculations." (González and Fiorito, 2015, pp. 560).

The first decade of the 21st century has seen multiple advances in the numerical analysis of the overall performance of daylight spaces, according to Mardaljevic et al. (2009). These advances include more refined glare prediction and simulation methods, distribution of natural light and radiation analysis. These innovations stand in harsh contrast to current daylighting design practice, which, according to Reinhart and Wienold (2011), "still favors the use of rules of thumb during schematic design and largely relies on the daylight factor" (Reinhart and Wienold, 2011, pp. 386) and illuminance distributions under unreal circumstances of clear sky conditions during solstice and equinox days.

Regarding model simulation, according to Agirbas (2017), "[...] [they] can be described as an experimental environment which, depending on the time, enable inferences to be drawn on the basis of exact or approximate information" (Agirbas, 2007, pp. 325).

Krüger and Laroca (2010) state that, over the first decades of the 21st century, several research works focused on the simulation and evaluation of small systems or individual systems in a building. "In tropical and

subtropical climates, the thermal performance evaluation [...] should be primarily related to the optimization of indoor comfort conditions [...]" (Krüger and Laroca, 2010, pp. 661).

Over the past twenty years, the creation of shading devices, regardless of the face of the building, was manual, and variations such as latitude, longitude, building rotation, geometry modification and others, required analog rework. According to Eltaweel and Su (2017), in the contemporary conception of architecture, all these aspects can be considered parameters and with the application of the correct software, it is possible to assemble a complete base, which can be altered and improved efficiently, so that the design of the building simultaneously changes without rework.

The term parametric originates from mathematics, and refers to using certain parameters or variables, which can be amended in order to manipulate with the equation results. Eltaweel and Su (2017) state that,

[...] the principle of parametric design can be defined as mathematical design, where the relationship between the [...] elements are shown as parameters, which could be reformulated to generate complex geometries. [...] By changing these parameters, new shapes are created simultaneously. (Eltaweel and Su, 2017, pp. 1087)

The integration of parametric design with performance simulation tools gave the user the ability of testing, comparing and selecting the best solution for multi-objective problems, as the ones found in the built environment (González and Fiorito, 2015).

Nowadays, parametric design is used in many fields, disciplines that consist of complex algorithmic relations, interdisciplinary work, creative forms, and multiprocessing treatments. [...] Due to this advancement in our life, we can find many implementations of parametric design in many fields like decoration, fashion, architecture, urban planning, sonic study, structural analysis, medicine and so on. (Eltaweel and Su, 2017, pp. 1090)

In architecture, according to Eltaweel and Su (2017), parametric design can generate creative solutions, deal with sophisticated relations and control them parametrically. It utilizes parameters to set relations between design elements in order to define a range of formal alternatives. It can also calculate algorithmic formulas and manipulate complex connections, besides creating sophisticated relations with several kinds of materials.

Andrade and Ruschel (2009) have identified that publications on the use of parametric modeling programs have emerged in the first decade of the 21st century in national congresses and events. Santana et al. (2015) infer that, although parameterization has been applied to energy efficiency studies for almost two decades in Brazil, the evaluations that take into account shape parameters are a novelty, due to the computational advances implemented in the 2010s.

2.3. Complex roof covers

According to Lebeé (2015), the concept of folding covers many significations. In nature, it can be related to specific shapes such as creases or pleats and may be found at different scales from the folding of graphen layers, to the unfolding of leaves and mountains (orogeny). "Pleated fabrics found on Egyptian frescoes prove that, long ago, mankind also handcrafted folds. However, the abstract idea of a folded surface emerged rather recently" (Lebeé, 2015, pp. 55).

When it concerns to the materialization of the parametric form, Pesenti et al. (2015) point out the kinematics potential of Origami creased patterns and investigate how those geometries can be modelled to optimize its surface displacements. Thus, the kinetics exploration is developed through the achievement of different ways to fold the surface.

"From Ori meaning 'folding', and kami meaning 'paper', the Origami, has evolved over the centuries from a traditional Japanese folk art to a design strategy for contemporary architecture and products" (Hemmerling, 2010, pp. 89). Origami is the art of folding, or more formally, "isometrically transforming, a sheet of paper into various forms without stretching, cutting, or gluing another piece of paper to it" (Tachi, 2010, pp. 203). Using origami, a complex 3D shape can be produced; hence, it can be applied for forming the shapes of a variety of architectural elements so that there is no need to assemble multiple parts.

Hemmerling (2010) states that the basics of the origami folds include valley and mountain folds, pleats, reverse folds, squash folds, and sinks. The number of basic folds is small, but they can be combined in a variety of ways to make intricate designs.

The use of Origami at different levels fits Origami patterns into several engineered applications; as deployable and reconfigurable structures, folding geometries have been used in biomedical devices, in space and aircraft applications. According to Pesenti et al. (2015), however, the use of self-folding Origami in architecture is mainly experimental, especially regarding shading devices and facade applications.

Since the form finding, geometry guides the project through the optimization of the shape, implementation of parameters, assembling circumstances and execution process.

Tachi (2010) strongly criticizes the fact that, when applying Origami to real life designs, it is important to control the customized 3D shape so that the resulting folded state is consistent with the required functionality, existing structures and environments. Therefore, according to Tachi (2010), computationally constructing an arbitrarily formed 3D surface using origami is a challenge to origami artists, architects, engineers, designers and personal users who apply origami to practical purposes.

According to Pesenti et al. (2015), a reason for choosing Origami as a process to develop shading screens is the spontaneous self-organization of these particular geometries, considered as an intuitive way to perform adaptation.

In fact, thanks to tessellation's creases, the Origami folding patterns enable the system to deform easily into a preset deformation direction, while remaining stiff in the other directions. These systems are capable of changing their shape to accommodate new requirements while maintaining a continuous external surface, as quoted by [Peraza-Hernandez et al. \(2014\)](#).

There is a deep connection between origami and mathematics, which has given rise to a new theoretical field of research in recent decades, called origami mathematics. [Lebe  \(2015\)](#) states that origami provides more possibilities than the classical Euclid axioms, since trisecting an angle is not possible with rule and compass, but can be done with folding.

[Hemmerling \(2010\)](#) also states that a considerable amount of mathematical study has focused on the art of Origami, since it is related to geometric principles. "The knowledge of geometric rules is at the same time an essential condition for the development of architecture in the design as well as in the realization process." ([Hemmerling, 2010](#), pp. 90).

As reported by [Lebe  \(2015\)](#), rigid folding is the most used and researched pleat. It happens when all the deformation is focused on the hinges, while the faces between the pleats remain flat. The curved folds are a more general class of pleats. In this case, the fold line is not straight. This rather simple generalization of folds actually generates a much more complex understanding of folding. Clearly, the surface is no more rigid-foldable.

Since folding is certainly the most simple and inexpensive process for transforming matter, it is a good starting point for design. Its process enables fast and easy achievement of three-dimensional shapes, which shows better structural properties than the original sheet and directly defines an envelope, separating the "inside" from the "outside".

According to [Peraza-Hernandez et al. \(2014\)](#),

In the mid-1970s, mathematicians discovered that an endless number of shapes could, in theory, be created using traditional origami (initially planar shape, only folds allowed). These discoveries enabled new approaches for manufacturing, assembling, and morphing of devices and structures based on origami principles. This is evident in the increasing attention mathematicians, scientists, and engineers have given to origami theories and tools over the past four decades. ([Peraza-Hernandez et al., 2014](#), para. 2)

[Peraza-Hernandez et al. \(2014\)](#) state that Origami offers designers novel ways to fabricate, assemble, store, and morph structures. Potential advantages include the ability to compactly store structures, reconfigure structures and reduce manufacturing complexity. It provides a quick response to the urgent request of building a structure. It is viable to create an outer skin or a canopy in a single operation, using pre-fabricated structures, working directly in a whole structure, rather than in every single element, which reduces assembly time. It even gives immediate structural logic, and all the pieces are linked to each other ([Mattoccia et al., 2016](#)).

Today, the combination of parametric tools, new fabrication and prototyping processes based on numerical

control and 3D printers brings architects and designers even closer to actual constructions.

Three patterns are particularly interesting: Yoshimura pattern, Miura Ori pattern and Diagonal pattern. All three are based on a combination of simple accordion folding and reverse fold, which means that they are a series of straight valley and mountain folds bent in the reverse folds to form simple curved surfaces ([Fig. 1](#)).

According to [Lebe  \(2015\)](#), Miura Buckling is the most investigated pattern. The homogenized behavior of the pattern alone was studied, as well as its behavior when used as the core of a sandwich panel. Many generalizations of the pattern were suggested, which are under current investigation.

According to [Gilewska et al. \(2014\)](#), folded plates¹ are also an attractive solution for architects and there are a lot of interesting engineering structures of this kind. Considering its aesthetic results, along with its easy generation through parametric modeling tools, it is believed that this type of geometry of Origami engineered structures will be increasingly used in contemporary buildings, which justifies its study.

2.3.1. Yoshimura pattern (diamond pattern)

According to [Hoff \(1966\)](#), this buckling pattern is named after Yoshimaru Yoshimura, the Japanese researcher who first provided an explanation for its development in a paper published it in Japan in 1951, and later republished in the United States.

The basis of this pattern ([Fig. 2](#)) is a diamond shape, fold in one of its diagonals. In the Figure, blue lines represent mountains and red dotted lines represent valleys. The Japanese scientist observed that thin walled cylinders show this kind of buckling pattern under axial compression ([Buri and Weinand, 2008; Hunt and Ario, 2005](#)). This pattern (also referred to as the diamond pattern) is constructed by repeating a single 6-degree vertex with mirror symmetry.

Another variation of this pattern can be obtained by splitting the diamond, or kite shape, and stretching it along the folded diagonal. The result is a hexagonal pattern formed by symmetrical trapezoids.

The diagonals of the diamond are equivalent to the main crease of the reverse fold and the edges of the diamond to the side creases. The curve of the folded pattern is designed by the shape of the diamonds. "The acuter the angle α between the diagonal of the diamond and its edge, the flatter the bending of the pattern." ([Buri and Weinand, 2008](#), para. 6).

According to [Chudoba et al. \(2014\)](#), the Yoshimura crease pattern takes on shapes with a single curvature at any intermediate stage of folding. The shapes achieved in this form are well known in architecture. They are assembled using triangular elements of the same size.

¹ "From mechanical point of view the correct theory to describe folded plates is six parameter shell theory with three displacements and three rotations in the displacement field. The third rotation is necessary because of folding the structure. Each fold is flat, so the equations of the theory can be simplified." ([Gilewski et al., 2014](#), pp. 220) They are assemblies of flat plates, rigidly connected along their edges in a way that the structural system is capable of carrying loads without the need for additional supporting beams.

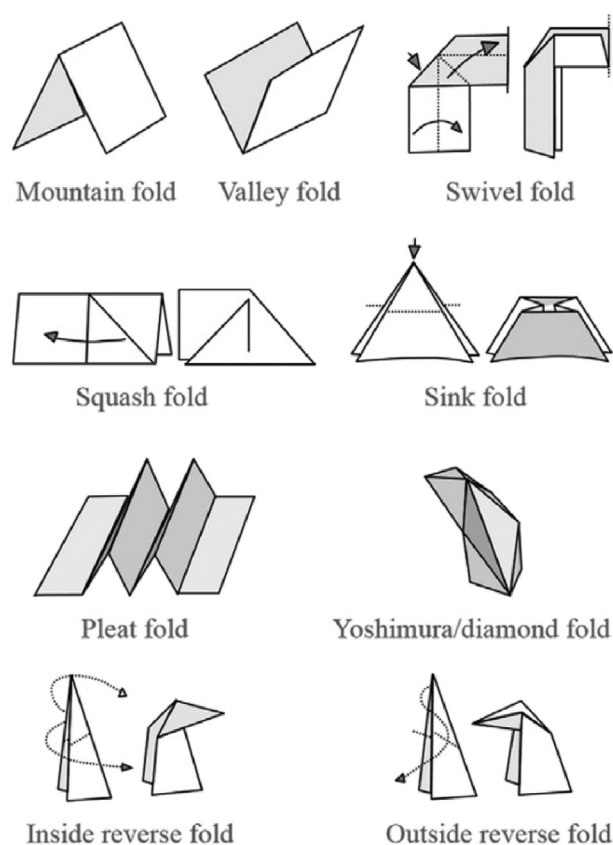


Fig. 1 Basic origami folds and techniques. Source: Redrawn from Gilewska et al. (2014).

The individual facets remain rigid when the buckling is not folded proportionally and are not imposed to any deformation at any stage of the folding process.

Chudoba et al. (2014) also state that its global curvature can be varied by changing the relation between the crease line length in both directions and by scaling the Yoshimura elements, so that their sides have different lengths.

2.3.2. Diagonal pattern

According to Buri and Weinand (2008), the basis of this pattern is a parallelogram folded in its diagonal, (Fig. 3), where the blue lines represent mountains and the red

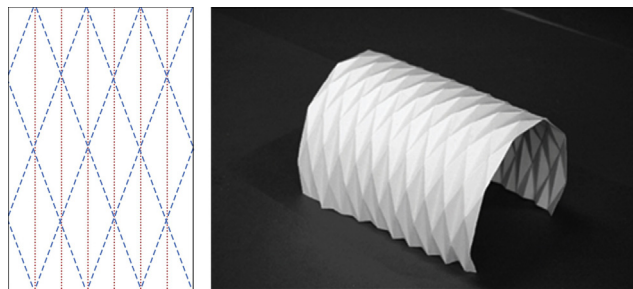


Fig. 2 Yoshimura buckling. Source: The author; Buri and Weinand (2008).

dotted lines represent valleys. Out of a parallel position, the edges are turned up diagonally. A series of folded parallelograms form a helical distorted folding. "A similar buckling pattern appears when a thin walled cylinder shell is compressed with a distortion" (Buri and Weinand, 2008, para. 7).

According to Buri and Weinand (2008), the Diagonal and the Yoshimura "mainly differ by the fact that valley folds of diamond pattern form a plane polygonal line whereas the valley folds of the diamond pattern form a helical polygonal line" (Buri and Weinand, 2008, para. 7).

2.3.3. Miura Ori pattern

According to Nishiyama (2012), the Miura fold (Fig. 4), is a method of folding named after its inventor, Japanese astrophysicist Koryo Miura.

Bain (1980) states that the crease patterns of the Miura fold form a tessellation of the surface by using parallelograms. In one direction, the creases lie along straight lines, with each parallelogram forming the mirror reflection of its neighbor across each crease. In the other direction, the creases zigzag. "Each of the zigzag paths of creases consists solely of mountain folds or of valley folds, with mountains alternating with valleys from one zigzag path to the next." (Bain, 1980).

Nishiyama (2012) says that this fold is a form of rigid Origami, which means that it can be carried out by a continuous motion in which, at each step, each parallelogram is completely flat. This property allows it to fold surfaces made of rigid materials.

According to Miura (1985), this pattern was employed due to its ability to be used in the construction of solar sails for satellites that could be packed in a very compact way and have maximum extension when unfolded (Buri and Weinand, 2008). The pattern is composed of symmetric trapezoids that form a herringbone tessellation.

3. Research methodology

3.1. Form selection

Taking into consideration the applications of the Miura Ori Tessellation form, altogether with its adaptability and free-standing characteristics, this was the pattern chosen for the construction of the parametric form. Among the patterns presented, the Miura-Ori pattern was selected due to its rigidity, easy motion and freestanding characteristics. The folded pattern has a zigzag feature in two directions, which allows extending and retracting the pattern in both directions.

Any thin horizontal surface can cover a large span, but will bend under its dead weight. The folds give the surface the resistance to support loads. Each inclined face of the folded surface functions as a beam, which is horizontally supported by the adjoining face.

3.2. Form parameterization

According to Buri and Weinand (2008), the form of parallel corrugations can be manifold. Extension is the main parameter characterizing a series of parallel folds. It can define the direction and magnitude of the deploying creases. The either chosen direction can be straight, bent or

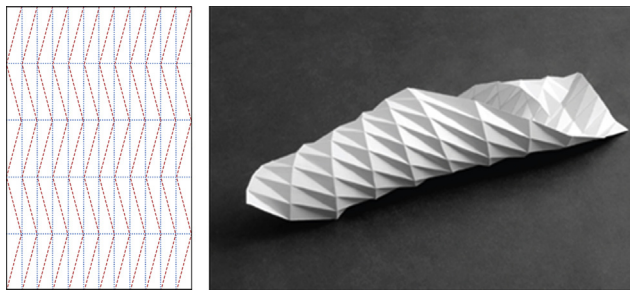


Fig. 3 Diagonal buckling. Source: The author; [Buri and Weinand \(2008\)](#).

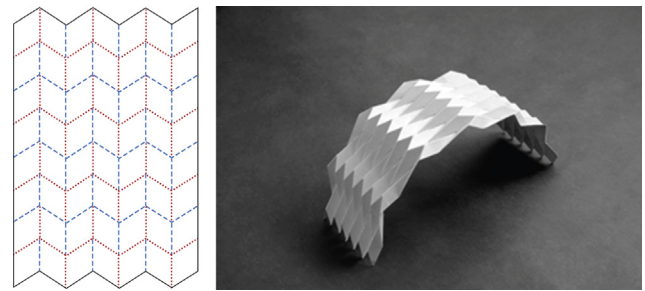


Fig. 4 Miura Ori buckling. Source: The author; [Buri and Weinand \(2008\)](#).

take an arbitrary curvilinear or polygonal form. The magnitude may vary between an entirely closed and a completely opened state. Extension length and amplitude vary according to the chosen magnitude. Other typical variation is the amplitude constant growth or reduction. Local or general variations of amplitude can be used to adapt the folded plate structures to stress. The higher the amplitude, the stronger the resistance of the folded plate structure. The order of mountain and valley folds does also qualify the appearance of a series of parallel folds.

The most basic folding is a corrugation of parallel mountain and valley folds. It can be described as an extrusion of a zigzag line along a straight line. The zigzag is characterized by the extension and the amplitude of its segments.

Using the Rhinoceros3D® and Grasshopper® parametric modeling suite, a solar protection element using Miura-Ori Buckling pattern was created.

Using the Rhinoceros3D® and Grasshopper® parametric modeling suite, a solar protection element using Miura-Ori Buckling pattern was created.

This choice is based on the idea of exploring the potential of the modeling tools, besides investigating the behavior of complex surfaces² applied as shading device.

In order to establish the cause and effect relationships between the geometry and performance of the developed shading elements, the following geometric parameters of variation between the models were defined: Number of Modules, Scaling of Modules, Deviation or Angulation and Aperture.

In order to obtain a foldable surface, the methodology used was extracted from [Mattoccia et al. \(2016\)](#). The main steps of the algorithm ([Fig. 5](#)) are listed below:

- (1) Defining a starting point A;
- (2) Defining a line AB, giving the starting point A, its length and the azimuth angle A'AB;
- (3) Defining a second line BC giving the starting point B, its length and two angles, the vertical one B''BC and the horizontal one B'BC;

² According to [Paoletti \(2006, our translation\)](#), complex surfaces are those that appear as fluid, formed by spherical solids in order to create curved volumes or volumes with complexity in their morphology and material, maintaining close relation with information technologies and, above all, with junction of a great number of responsibilities and competences, aiming to organize the constructive processes.

- (4) Defining the first starting plane ABCD, giving the two previous lines and the inner angle BCD;
- (5) Defining a third line giving the starting point B, its length and the vertical angle B''BE;
- (6) Defining the second starting plane BCDE, giving the line BC and BE and the inner angle BCF;
- (7) Find the other two planes of the smallest constituent component CDHI and CHGF using the relation about the dihedral fold angles which are related to the previous inner angles BCD and BCF;
- (8) The last step, according to [Mattoccia et al. \(2016\)](#) is to continue the surface in the transverse direction, getting the two new planes EFML and MFGN.

Having the object divided into planes allows resizing of the module at any time, as well as increasing the number of modules in the X or Y-axis ([Fig. 6](#)).

As it can be seen, 3 Number Sliders are responsible for the scale of the model. The X Length one is responsible for scaling the module in the X-axis. Deviation, despite being connected to the Y-axis, is responsible for the angulation and deviation in the Y-axis, making the model angles more or less acute.

The Y Length, on the other hand, is responsible for scaling in the Y-axis. There is also an X and Y count controlling the number of modules in each axis.

The main module was constructed in the XY plane ([Fig. 7](#)) and an original folding asset is created and maintained at 100 to prevent deformity. A folding asset is created to simulate the plate foldability. It ranges from 0.00 to 0.99, so that 0.00 is a flat surface, with no buckling, and 0.99 is the Miura fold completely folded and retracted.

3.3. Factorial analysis for radiation output

According to [Montgomery et al. \(2012\)](#), the Factorial Analysis is an alternative to discover interactions between the variables. Experimental planning is a technique based on defined scientific and statistical criteria, with the purpose of determining the effect of the variables on the results of a given process.

According to [Ferreira \(2016\)](#), in the Factorial Analysis, all factors³ are varied together. The number of factors

³ Linear combination of the original variables, forming statistical variables to maximize their power, in order to explain the complete set of variables ([Hair et al., 2005](#)).

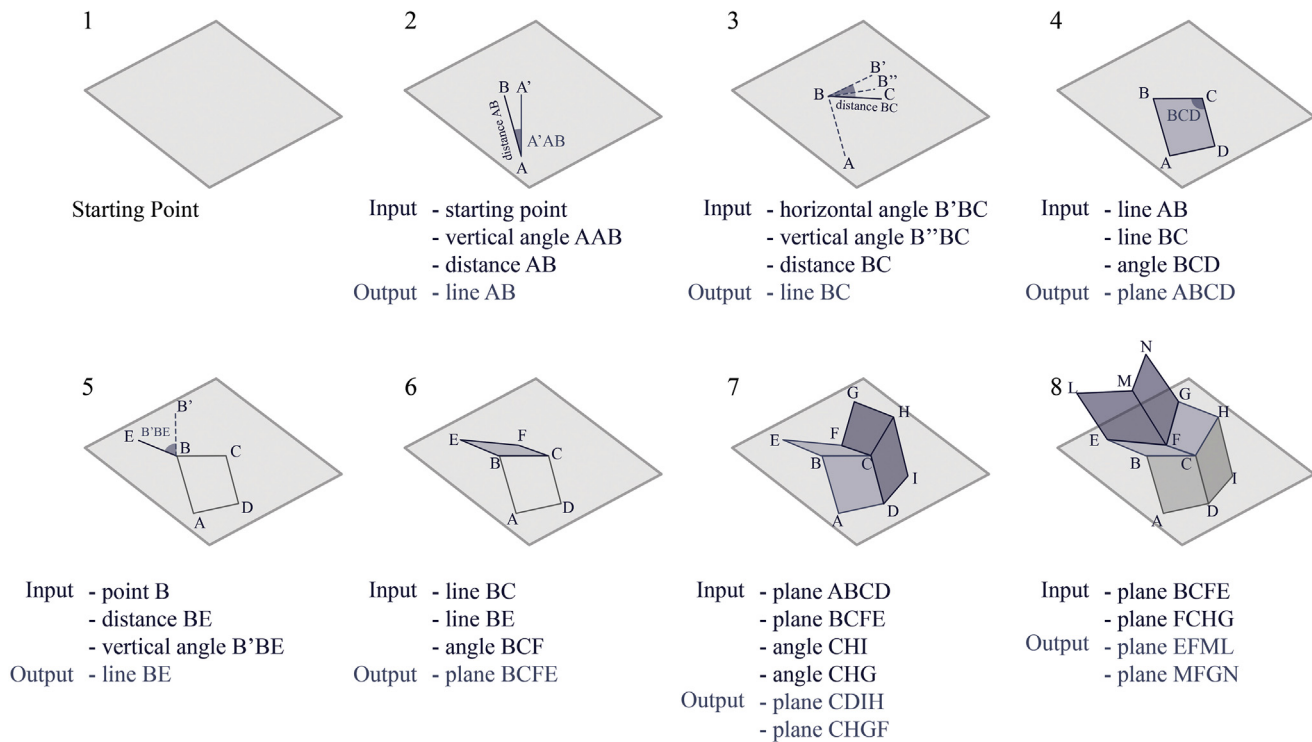


Fig. 5 Steps followed in Grasshopper. Source: [Mattoccia et al. \(2016\)](#).

will depend on the number of variables and levels of experimentation. The simplest type is factorial, $2k$. The terminology derives from the fact that only two levels for each factor k are assumed. One indicates the low level, represented by a minus (-) and the high level, represented by a plus (+), or indicates the presence or absence of a factor. Besides, each factor level combination can be tested more than once in order to minimize the effect of random errors, which is called replica ([Reddy, 2011](#)).

The replica is usually applied in experiments with many factors or a lot of information to process. To avoid making the experiment impracticable due to its size, it is run at two levels at maximum, according to [Pinto \(2003\)](#). [Montgomery et al. \(2012\)](#) state that there are no restrictions regarding the amount of factors and levels that a factorial design may contain. The factorial experiments adopted were two levels for cardinal orientations and collateral orientations ([Tables 1 and 2](#)). The simulation outputs of Annual Average of Hourly Radiation were used in the Factorial Analysis.

The effect of each variable on the process is delimited by means of controlled changes in the process and evaluation of the impact on the results, or the output data, obtained in the interactions. We use the Variance Analysis (ANOVA) techniques to identify statistically robust models with good performance between the response variable and the various factors. The analysis of variance allows evaluating the degree of reliability of the measures obtained, that is, if the effects are significantly different from zero. In particular, ANOVA tests whether several populations have the same mean by comparing the dispersion of the

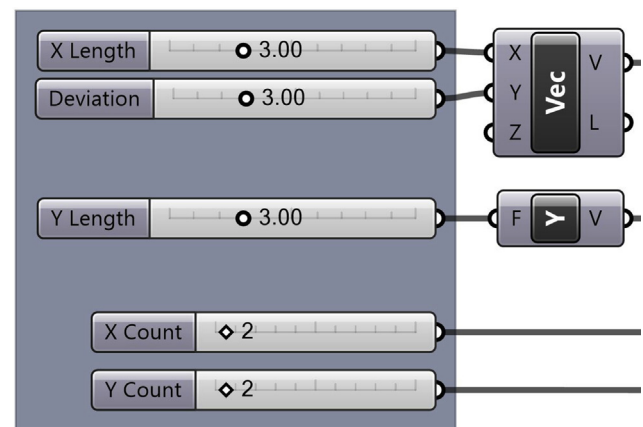


Fig. 6 Input parameters for canopy and modules size. Source: The author.

sample means with the variation within the samples ([Montgomery et al., 2012](#)).

For this study, the factorial analysis was applied to determine the most sensitive parameters applied to the canopy.

From the experiments, the simulations and their corresponding outputs are defined and used as output variables of the factorial analysis, which will be later statistically treated by analysis of variance (ANOVA).

After the definition of the levels of the parameters and the output variable, the factorial experiment was elaborated and the simulations were run to obtain the Annual Average of Hourly Radiation, used as the main output variable.

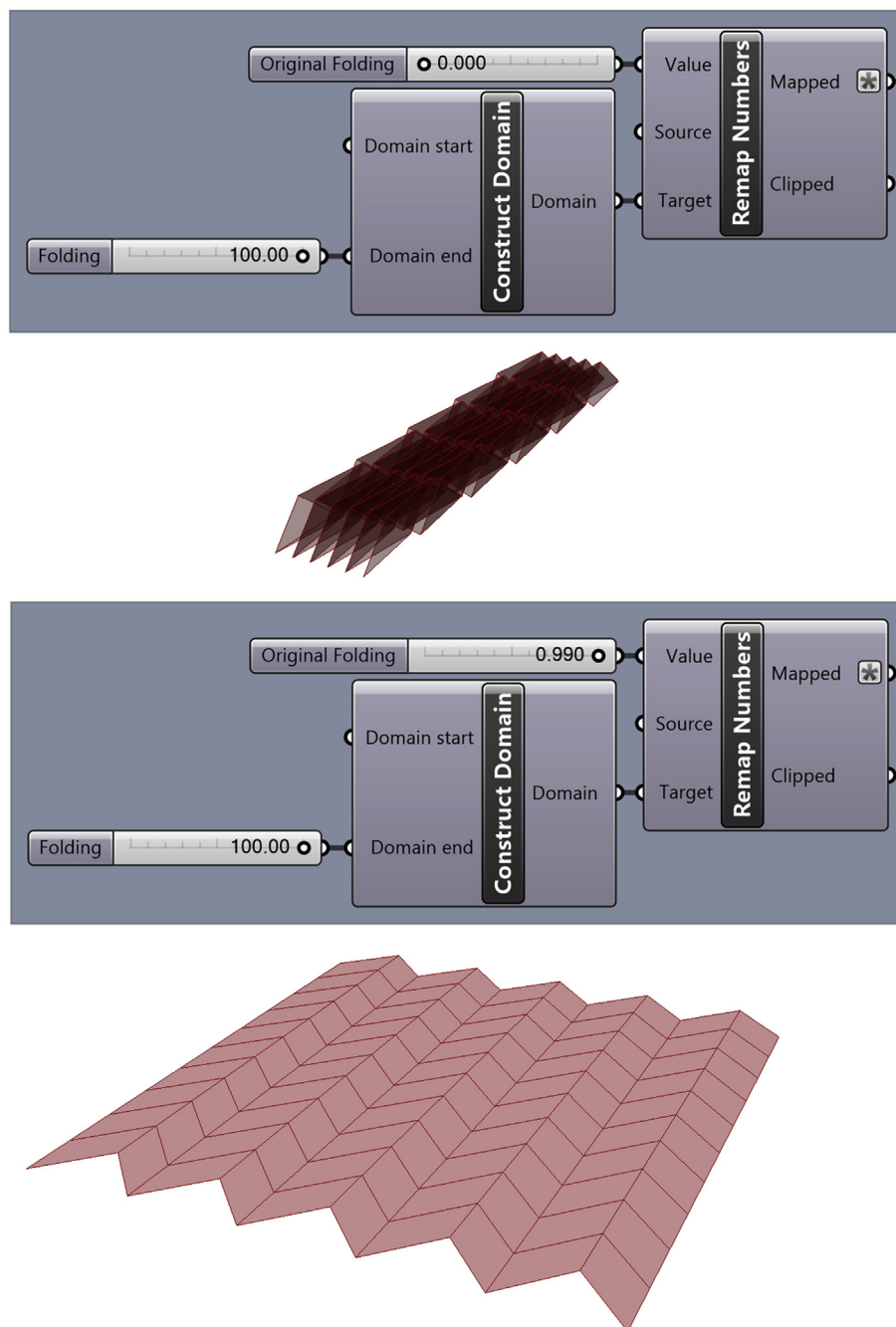


Fig. 7 Parameters for Folding and their impact on the Canopy. Source: The author.

3.4. Simulation

The plug-in LadyBug® for Grasshopper® was selected for radiation analysis, Operative Temperature (T_o) and Percentage of Time in Comfort (PTC), since, according to Roudsari and Pak (2013), Ladybug® imports standard EnergyPlus Weather files (.epw) into Grasshopper® plug-in and provides a variety of 2D and 3D interactive graphics to support the decision-making process during all stages of design. It also simplifies the process of analysis, automates and expedites the calculations and makes it easy to understand and manipulate graphical visualizations in the 3D

modeling interface of Rhino/Grasshopper®. "It also allows users to work with validated energy and daylighting engines such as EnergyPlus, Radiance and Daysim" (Roudsari and Pak, 2013, pp. 3129).

The plug-in HoneyBee® for Grasshopper® was used for ASHRAE Adaptive Comfort Calculations. According to Roudsari and Pak (2013), Honeybee® is an extension of Ladybug® that increases the ability to work with Radiance, Daysim or EnergyPlus. "Similar to Ladybug®, Honeybee® is designed to run the analysis on building masses but for more advanced [lighting] studies" (Roudsari and Pak, 2013, pp. 3132).

Considering the need to measure the levels of Total Radiation and obtain the Annual Average of Hourly Radiation, a plan needs to be created just below the structure of the Canopy. The plane created below the canopy should be smaller than the Canopy so as to be affected by the shadows cast by the object and collect the least amount of solar radiation unaffected by the canopy. Following the methodology applied by [Cartana et al. \(2018\)](#) for radiation simulation, the horizontal plan was created 10 cm aloof from the canopy alignment, with sensors spaced by 20 cm \times 20 cm.

In this stage, the Radiation analysis plan just below the structure will be used as the main assessed geometry while the Canopy will be inserted separately as a context geometry.

The simulation was performed for a full year using the weather file TMY3 ([Guimarães, 2016](#)) for Viçosa, MG (Latitude 20° 45' 14" S, Longitude 42° 52' 55" W, Altitude 648 m). Since the canopy is parameterized, the simulations work adequately for any other place, with different solar radiation, depending only on the weather file inserted.

The canopy was chosen because in places with hot and humid climates, such as Brazil, the roofing areas are critical parts of the building envelopes and "highly susceptible to solar radiation and other environmental changes, thereby, influencing the indoor comfort conditions for the occupants" ([Sadineni et al., 2011](#), pp. 3622).

4. Analysis

4.1. ASHRAE 55 adaptive comfort and Percentage of Time in Comfort (PTC)

According to [Lamberts et al. \(2013\)](#),

since there was no Brazilian thermal comfort standard available for workplaces, studies carried out during the 1990's and 2000's were vastly influenced by the ISO 7730's procedures, which is based on Fanger's [predicted mean vote/predicted percentage of dissatisfied] PMV/PPD equation. ([Lamberts et al., 2013](#), pp. 19)

[Lamberts et al. \(2013\)](#) discuss that, although studies were affected by ISO 7730, the few research works attempting to establish thermal comfort zones across different climatic zones in Brazil revealed significant differences regarding the percentage of people dissatisfied with the use of Fanger's PPD, particularly in hot and humid climates. This is observed mainly because "occupants in naturally ventilated buildings

Table 2 Levels for the collateral factorial experiment.

Factor Level	Factor A		Factor B		Factor C
	Cardinal Rotation		Collateral Rotation		Slope
Low (–)	South		West		5°
High (+)	North		East		20°
Factor	A	B	C	Description	
(1)	–	–	–	Southwest 5°	
a	+	–	–	Northwest 5°	
b	–	+	–	Southeast 5°	
c	–	–	–	Southwest 20°	
ab	+	+	–	Northeast 5°	
ac	+	–	+	Northwest 20°	
bc	–	+	+	Southeast 20°	
abc	+	+	+	Northeast 20°	

accept temperature swings during the day and year, and prefer higher air velocities if controls and fans are provided." ([Lamberts et al., 2013](#), pp. 22).

In this scenario, the latest version of [ASHRAE Standard 55 \(2013\)](#) "emerges as the best inspiration for any thermal comfort standard worldwide" ([Lamberts et al., 2013](#), pp. 24). The Standard defines acceptability limits of 80% comfort for typical applications and 90% comfort when a higher standard of thermal comfort is desired. It indicates the percentage of occupants expected to be comfortable at the indicated indoor and prevailing mean outdoor temperatures ([Table 3](#)).

According to [de Dear and Brager \(1998\)](#), the adaptive comfort adopts varying internal temperature standards and allows users to adapt to the environmental conditions of the building. This approach leads to more responsive environmental control algorithms, improved levels of occupant comfort and reduced energy consumption, besides promoting sustainable projects.

The adaptive comfort considers the human body as an active agent that interacts with the environment in response to its preference and thermal sensation. It is based on a broad sampling of field studies conducted in various parts of the world, whose indexes are based on results that measure environmental conditions and the simultaneous response to thermal sensation in individuals involved in their usual tasks ([de Dear and Brager, 1998](#)). The researches seek to reproduce the real conditions, where the users of the building are active agents in the thermal conditions of the environment. Besides, the populations of different climatic regions, socio-cultural and

Table 1 Levels for the cardinal factorial experiment.

Factor Level	Factor A		Factor B
	Cardinal Rotation		Slope
Low (–)	South		5°
High (+)	North		20°
Factor	A	B	Description
(1)	–	–	South 5°
A	+	–	North 5°
B	–	+	South 20°
Ab	+	+	North 20°

Table 3 Acceptability and applicability ranges of adaptive comfort model. Source: ASHRAE 55 2013 Standards.

Acceptability Limits	Air Velocity (m/s)	Activity level (met)	Clothing Insulation (clo)	Operative Temperature (°C)	
				Summer	Winter
80%	<0.2	1.0–1.3	0.5–1.0	30.3	23.3
90%	<0.2	1.0–1.3	0.5–1.0	24.3	24.3

socioeconomic contexts have different perceptions of comfort, as reported by [Pereira and Assis \(2010\)](#).

The thermal performance of the space can be evaluated using Total Comfortable Hours (TCH) followed by Percentage of Time in Comfort (PTC), Percentage Hot (PH), Percentage Cold (PC), and Adaptive Comfort (AC) (also called condition of person), where the input conditions are: -1 cold; 0 comfortable; +1 hot for occupants.

According to [Abdullah and Alibaba \(2018\)](#), Ladybug Adaptive Comfort Calculator measures TCH, PTC, PH, PC, and AC values, whereas an adaptive comfort chart can be generated using the Ladybug Adaptive Comfort Chart.

ASHRAE 55 Adaptive comfort is applicable for the determination of the comfort indices in naturally ventilated environments, where the physical activity of users is between 1.0 met and 1.3 met. The method also specifies that occupants can freely adapt their clothing to internal and/or external thermal conditions within a range of 0.5–1.0 clo and an average air temperature between 10 °C and 33,5 °C is adopted ([ASHRAE, 2013](#)). The standard also determines that the acceptance limit range for typical construction applications must satisfy 80% of the individuals.

4.2. Operative temperature (To)

ASHRAE 55 (2013) Standard defines operative temperature as the weighted average of Mean Radiant Temperature (MRT) and air temperature, since occupants tend to lose half of their body heat through radiation and the other half by air-related factors, such as air temperature and humidity. It is a primary metric by which adaptive comfort and thermal conditions are measured.

4.3. Thermal Comfort Percent (TCP)

According to [Abdullah and Alibaba \(2018\)](#), "Thermal Comfort Percent, as a metric to map spatial comfort, is the percentage of time where a given point in space appears inside the adaptive comfort range" ([Abdullah and Alibaba, 2018](#), para. 20).

TCP can be interpreted as a loss in comfortable hours and in comfortable space in the analyzed period.

5. Results

5.1. Factorial analysis

Initially, the input values obtained after simulation for radiation in Grasshopper® are presented for the canopy, taking into account the cardinal directions. The effects calculated by Minitab for each of the factors are presented in [Fig. 8](#) along with 10 replicas, each one relative to 36 days of the year. The output variable in this analysis is Annual Average of Hourly Radiation.

For this factorial configuration, 3 types of replica were tested. The first test presented 4 replicas, one for each season. The second presented 6 replicas, each one with 2 months. The 10-replica configuration produced a more robust model, with less error and did not compromise the simulation time, taking into account that in a 2-level

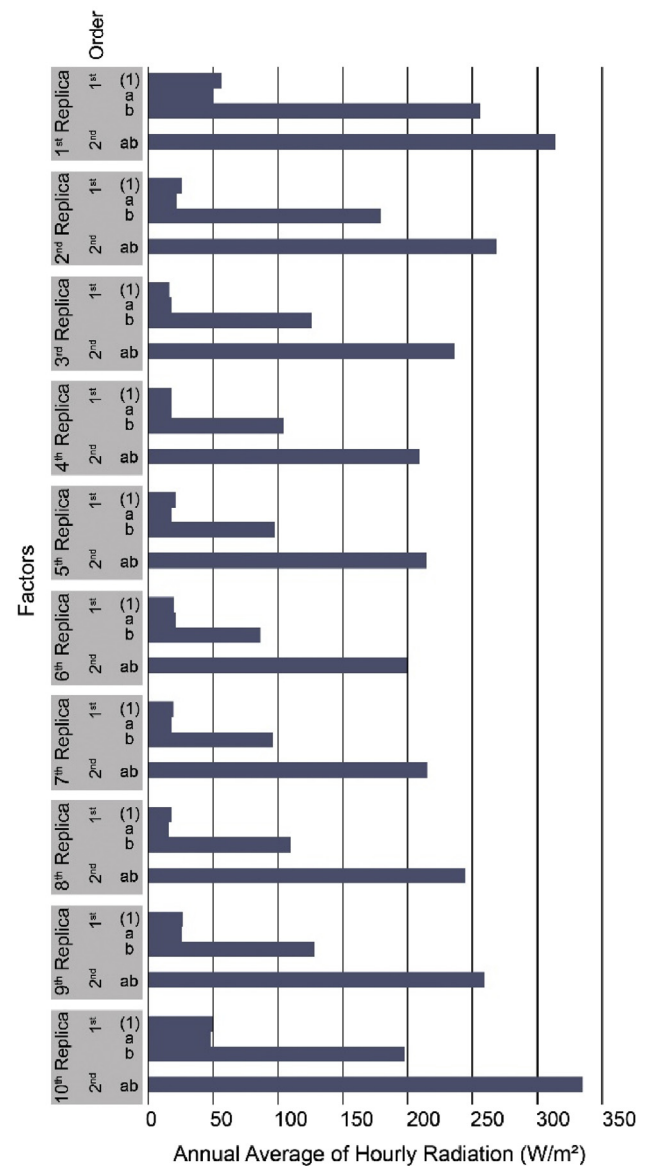


Fig. 8 Factors for factorial analysis and replicas for cardinal directions. Source: The author.

factorial, the number of tests is equivalent to 2^k multiplied by the number of replicas, where k is the number of factors.

For the Cardinal Analysis, the number of radiation simulations run was 40 ([Fig. 8](#)). It is observed that the level of Annual Average of Hourly Radiation is lower for Factors of the first order, more specifically for (1), which refers to

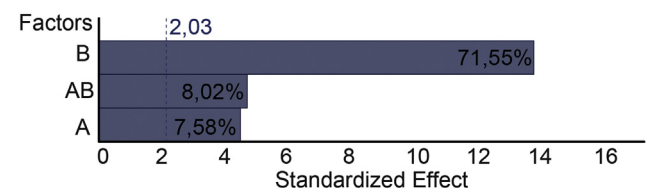


Fig. 9 Pareto chart of the standardized effect for cardinal directions. Source: The author.

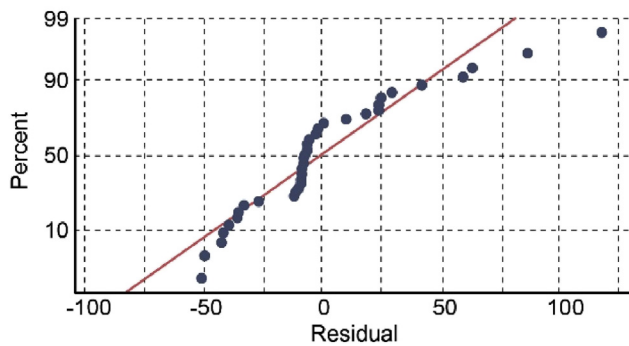


Fig. 10 Normal probability plot for cardinal directions. Source: The author.

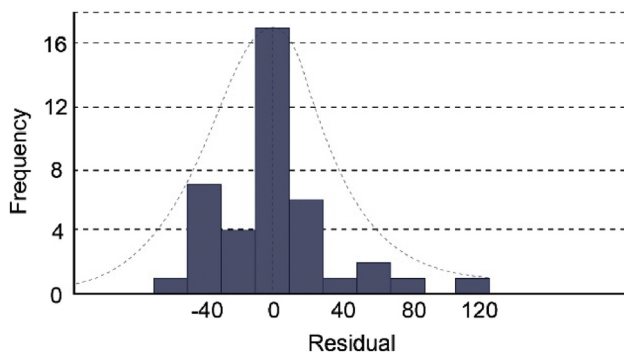


Fig. 11 Histogram for distribution of Normal for Cardinal Directions. Source: The author.

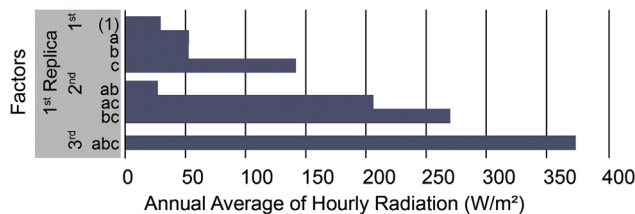


Fig. 12 Factors for factorial analysis for collateral directions. Source: The author.

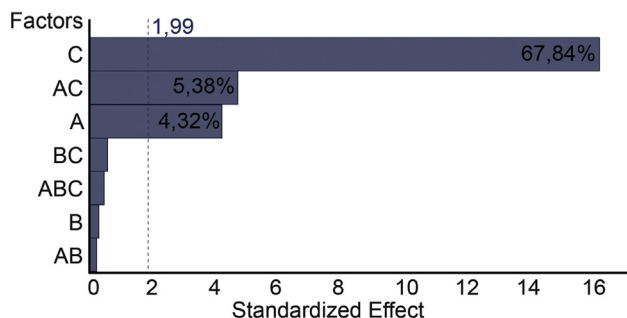


Fig. 13 Pareto chart of the standardized effect for collateral directions. Source: The author.

south 5°, and A, north 5°. It indicates lower levels of radiation for the plan below the canopy when it is less steep and little dependant on orientation.

The analysis of the output data obtained by simulation (Fig. 9) reveals that the cardinal direction alone is among the factors that least affect the model.

Factor a (cardinal rotation) contributed with 7.58%. However, the linear factor can still be considered interesting, even if it is lower than factor b, related to the slope of the canopy, which contributed with 71.55%, as well as the two-way interaction factor ab, related to the combination of factors (cardinal rotation and slope). Then, it can be concluded that the effect was representative for the case analyzed. Minitab shows a Model contribution of 87.15%. This indicates the occurrence of a 12.85% error embedded, which is acceptable. This error may indicate the existence of another important variable that has not been analyzed.

In a normal probability plot, the sorted data are plotted vs. values selected to make the resulting image look close to a straight line. Deviations from a straight line suggest departures from normality. The data distribution analysis (Figs. 10 and 11) shows that they follow such behavior, despite a slight deviation.

Normal distribution can also be analyzed by means of a histogram, which is an accurate representation of the distribution of numerical data. It is an estimate of the probability distribution of a continuous variable. The intervals must be adjacent. They often present the same size when the distribution is uniform. The histogram obtained through simulation for cardinal directions shows good normal distribution for the factorial experiment (Fig. 11), with slight deviation for positive values but roughly symmetric.

If the data distribution is not normal, or close to the normal, the effect calculation is a mean between the output variables obtained for the positive factors and negative factors. Thus, the means are no longer representative, but rather corrupted and tending to the stronger variables.

A 2-level factorial with 3 factors was created for the Collateral directions. The number of replicas remained the same, 10 replicas relative to 36 days for each year. Eighty radiation simulations were run.

The Factors graph (Fig. 12) shows the first replica, or the first 8 simulation results. In this experiment, it is observed

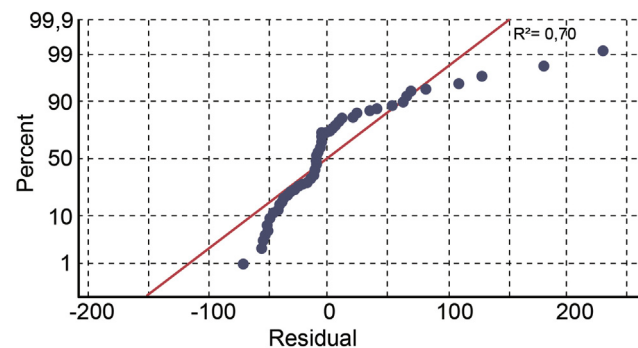


Fig. 14 Normal probability plot for collateral directions. Source: The author.

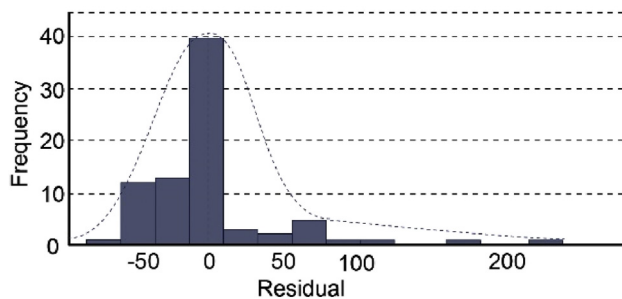


Fig. 15 Histogram for distribution of Normal for Collateral Directions. Source: The author.

that the level of Annual Average of Hourly Radiation for Factors of the first order is higher than those in the first experiment. However, the collateral and cardinal directions provided similar contributions. Factors of second and third order present even higher levels of Annual Average of Hourly Radiation, but only when combined with factor *c*, responsible for the slope.

The Pareto Chart for this factorial Analysis (Fig. 13) shows that factor *c* (slope) has the highest contribution, 67.84%. The correlation between the collateral direction represented by *a* and the slope represented by *c* is also an interesting two-way factor combination, which accounts for 5.38% of contribution to the factorial. Alone, *a* accounts for 4.32% of contribution, once the factor related to the slope had space to connect with other factors and increase its contribution proportionally. Minitab shows a Model contribution of 77.63%. This reveals a 22.37% error embedded, which is acceptable.

The highest error embedded in the model transmitted to the normal analysis. In the Normal Probability Plot (Fig. 14), it is observed a detachment from the normal, more pronounced than in the previous experiment.

This can be seen in the histogram (Fig. 15), which shows that the Normal is displaced, tending to the stronger values. The histogram presents two Outliers, which is an extremely high value that does not fall near any other data points. This can represent unusual cases, data entry errors, or perhaps data that do not belong to other data of interest. For this analysis, the residual values are left-skewed and the mean may not provide a

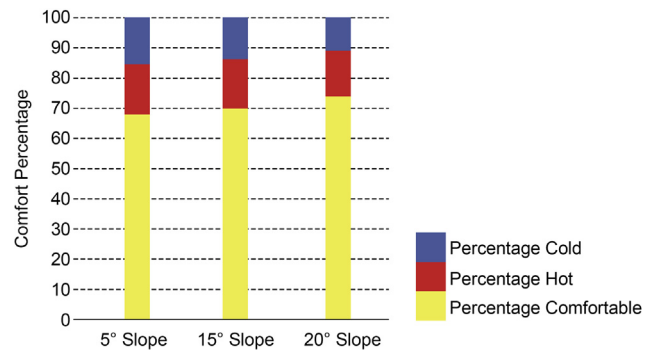


Fig. 17 Comfort percentage according to parameter change. Source: The author.

good estimate for the center of the data and represent where most of the data fall. In this case, the mean is typically less than the median.

5.2. Simulation analysis

As observed in the Factorial Analysis, the slope was the most robust factor analyzed and generated a higher level of differentiation between the radiation levels. Therefore, the North orientation was fixated for the model analyses and 3 different slopes were analyzed, 5°, 15° and 20°. The first is relative to a small slope on the canopy, only for water drainage. The second is relative to the equivalent angle for the minimum slope adopted in Brazil, which is 25%. The last one is an angle equivalent to the typical slope adopted in Brazil for ceramic roof tiles, which is between 30% and 38%.

5.2.1. ASHRAE 55 adaptive comfort and Percentage of Time in Comfort (PTC)

For the creation of the ASHRAE Adaptive Comfort for the Whole Year (Figs. 16 and 17), the space below the canopy was treated as one zone in HoneyBee®. For the zone Programming, it was treated as a natural ventilated hallway with fenestrations of 70% facing North and South and 50% facing East and West.

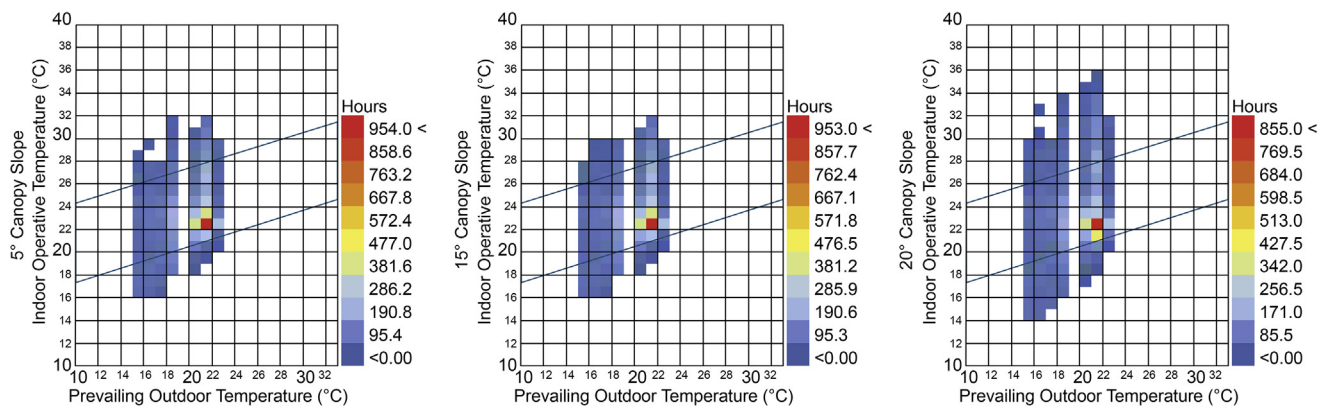


Fig. 16 Adaptive comfort chart for ASHRAE 55. Source: The author.

The adaptive comfort chart in Fig. 16 demonstrates the boundary of the comfort range for the 80% acceptability limit stated by the ASHRAE 55 standard.

This method defines a correlation between indoor operative temperature and prevailing outdoor temperature and explains that residents accept warmer degrees when outdoor air temperature rises. "The colorful squares represent the available comfort hours, for which the saturated colors in red contain a higher number of desired hours" (Abdullah and Alibaba, 2018, para. 29). The blue edged polygon indicates the adaptive comfort range.

The microclimate map visualizations show a significant thermal quality towards more comfortable space indoors and fulfil the intended acceptability limit of 80% for the ASHRAE (2013) Standards for 5°, 15° and primarily for 20°. The operative temperature was very close to the ideal degree almost at all points for most of the time when the analysis is carried out in percentage and the maximum shift is of 5 °C up and 3 °C down for the overall temperature for a natural conditioned space.

The thermal performance was evaluated using the adaptive comfort model (Fig. 16). The results showed that the total comfortable hours (TCH) were 5931 h, out of the 8760 simulated hours, in a year, for 5° slope. This number indicates that, in 67.7% of the total hours, the space was comfortable, corresponding to 32.3% of time in discomfort (PTD) (Fig. 18). The discomfort hours happened mainly between May and August, relative to fall and winter respectively, and predominantly before 8 AM. A critical comfort percentage was detected during the summer, mainly in March and the beginning of April, relative to fall.

The representation of Canopy slope of 15° was similar to that of 5°. Despite the visual representation, the data showed a TCH of 6132 h out of the 8760 simulated hours. This indicates a 70.0% of total comfort hours and corresponds to 30.0% PTD.

The results for 20° showed improvement when compared to the other slopes, as observed in Figs. 17 and 18. The simulation shows the percentage of 74.0% of comfortable hours, which accounts for a TCH of 6482 h out of the 8760 simulated hours and a PTD of 26.0%. The discomfort reported during the fall and winter (from March to September) is minimized and, besides the hours of discomfort in the middle of the year, due to cold, there is a small concentration of discomfort hours in the end of the summer (from December to March).

The ASHRAE Condition of a Person (Fig. 18) shows values for comfort or lack of comfort. Values of -1, for instance, are acknowledged to be cold and values of +1, hot. For 5° Canopy Slope, the Adaptive Comfort Calculation also indicates a percentage of 67.7% of comfortable time when dealing with inner spaces, with 16.7% PH and 15.5% PC, as observed in Fig. 17. For 15°, the simulation shows results of 16.2% PH and 13.8% PC. The best results were shown for 20°, with 15.4% PH and 10.6% PC.

5.2.2. Outdoor Shade Benefit

The Shade Benefit Chart for the whole year (Fig. 19) shows the benefit of shading with and without the 20° slope canopy application. As observed, the analysis of the shaded space reveals that the thermal condition of the space remains approximately within the adaptive comfort range of 25 °C, which is the lowest bound between 6AM and 6PM, during summer, and of 30 °C, which is the highest bound for the same time during the summer, based on the 80% acceptability limit of the ASHRAE 55 (2013) Standard. For the winter, the highest bound was 25 °C, which is within the adaptive range. The lowest bound was reported before 6AM, when the space is underused. Considering temperatures after 8 AM, the lowest bound reached 17 °C in June and July, which are winter months in Brazil. The results for 5° and 15° were very similar to those presented for the 20° slope.

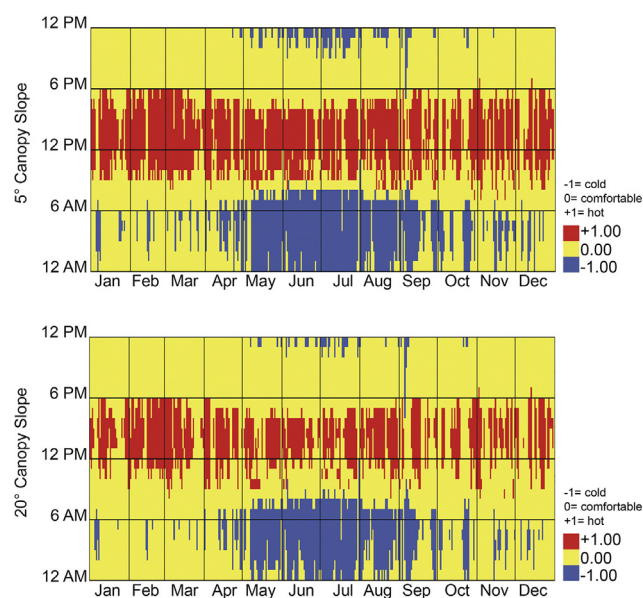


Fig. 18 ASHRAE 55 condition of a person. Source: The author.

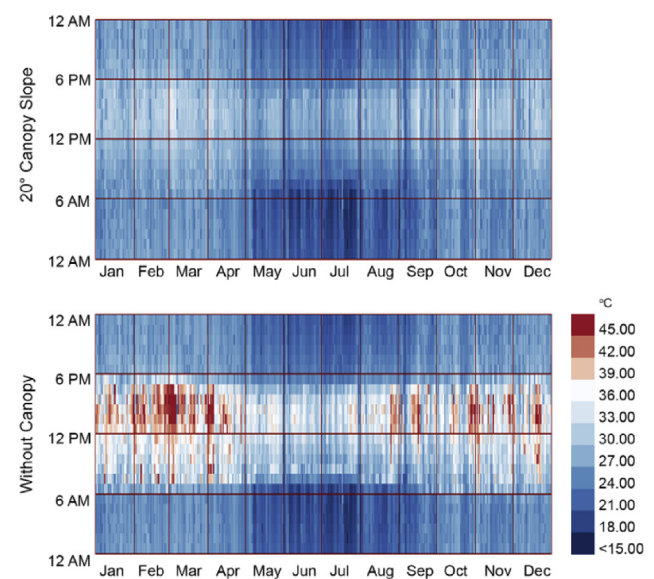


Fig. 19 Outdoor Shade Benefit for the whole year. Source: The author.

In the analysis of the space without the canopy, the temperature reached 45 °C in March and was consistently high throughout the summer months, from December to March. The temperature decreased slightly between May and August, relative to Fall and Winter, respectively. However, it was still higher than the range of $T_{comf} \pm 2.5$ °C for 80% Acceptability Limits during summer and winter.

The discomfort cold hours were mostly reported during the nighttime and before 6 AM, which did not noticeably affect the simulated analysis hours (08:00–18:00). However, due to the adiabatic walls adopted for the simulated model, which eliminates internal heat flows between the possible zones, the night times seemed colder than they actually were.

6. Conclusions

This study used parameterization, simulation and factorial analysis tools applied to a canopy created based on Origami techniques. Accessible digital simulation platforms were introduced and quantitative radiation analysis and qualitative radiation visualization were grinded in order to discover the most robust factors acting on the design of the canopy.

The paper presents a brief literature review on the origin, implementation and applications of Origami design in general and when it was specifically applied to a parametric design for radiation simulation.

The main purpose of this article was to create a complex parametric geometry based on Origami shapes and analyze some of the main factors with potential contribution to the incidence and transmission of Solar Radiation in the Canopy, using Factorial Analysis.

Among the main conclusions obtained, it is highlighted that, regarding the Factorial Analysis, the most robust factor observed in both analysis was a first order factor relative to the Canopy slope. The Canopy Orientation, although important to the conception of the model and somewhat representative, provided a smaller contribution. For the Cardinal Orientation Experiment, the Canopy Slope accounted for 71.55% of the total contribution, which was 87.15%. The second order factor accounted for 8.02%, relative to Slope and Orientation combined.

The analysis of the 5°, 15° and 20° slopes has proven that the differentiation of the inclination impacts the design, the amount of radiation received by the surface and the user comfort level.

The adaptive Comfort Model for 5° indicated a 67.7% total comfort hours with 16.7% PH and 15.5% PC. For the maximum slope of 20°, representative of a typical slope adopted in Brazil, the simulation shows a percentage of 74.0% of comfortable hours with 15.4% PH and 10.6% PC for a natural conditioned space.

A considerable part of the percentage of time in discomfort is related to hours before 8 AM mainly during winter and fall.

The results demonstrate that, together with the computational design technologies and the simulations available for the performance analysis of shading elements

with complex shapes, the understanding of the solar geometry is essential for a selective admission of solar radiation.

Although the simulation was run for Viçosa MG (Latitude 20° 45' 14" S, Longitude 42° 52' 55" W, Altitude 648 m), the parameterization allows it to be inserted anywhere else and the simulation requires only another weather file.

As an ongoing research, the next endeavor encompasses daylight evaluation and multi-objective optimization techniques to find trade-offs among different optimization objectives.

Acknowledgements

We are thankful to Fundação de Amparo à Pesquisa do Estado de Minas Gerais (FAPEMIG) for the scholarship granted.

References

- Abdullah, H.K., Alibaba, H.Z., 2018. Towards nearly zero-energy buildings: the potential of photovoltaic-integrated shading devices to achieve autonomous solar electricity and acceptable thermal comfort in naturally-ventilated office spaces. In: *Proceedings of the 16th International Conference on Clean Energy*. Famagusta: Eastern Mediterranean University.
- Agirbas, A., 2017. The use of simulation for creating folding structures: a teaching model. In: Fioravanti, A., Cursi, S., Elahmar, S., Gargaro, S., Loffreda, G., Novembri, G., Trento, A. (Eds.), *Proceedings of the 35th ECAADe Conference*. Sapienza University of Rome, Rome, pp. 325–332.
- Andrade, M.L., Ruschel, R.C., 2009. BIM: conceitos, Cenário das Pesquisas Publicadas no Brasil e Tendências. In: *Proceedings of the Simpósio Brasileiro de Qualidade do Projeto no Ambiente Construído*. São Carlos. Universidade de São Paulo, pp. 602–613.
- ASHRAE, 2013. ANSI/ASHRAE standard 55-2013. *Ashrae Standard 13*, pp. 431–439.
- Bader, J., Zitzler, E., 2011. HypE: an algorithm for fast hypervolume-based many-objective optimization. *Evol. Comput.* 19, 45–76.
- Bain, I., 1980. The Miura-Ori Map. *New Science*.
- Brotas, L., Rusovan, D., 2013. Parametric daylight envelope. In: *Proceedings of the PLEA 2013 -Sustainable Architecture for a Renewable Future*. Technische Universität München, Munich, pp. 304–322.
- Buri, H., Weinand, Y., 2008. ORIGAMI-folded plate structures, architecture. In: *Proceedings of the 10th World Conference on Timber Engineering*. Miyazaki: Engineered Wood Products Association.
- Cartana, R.P., Pereira, F.O.R., Mayer, A., 2018. Estudo piloto para elementos de controle solar desenvolvidos com modelagem paramétrica e fabricação digital. *Ambiente Construído* 18, 67–82.
- Cho, J., Yoo, C., Kim, Y., 2014. Viability of exterior shading devices for high-rise residential buildings: case study for cooling energy saving and economic feasibility analysis. *Energy Build.* 82, 771–785.
- Chudoba, R., van der Woerd, J., Hegger, J., 2014. Numerical modeling support for form-finding and manufacturing of folded plate structures made of cementitious composites using origami principles. In: Bićanić, N., Mang, H., Meschke, G., de Borst, R. (Eds.), *Proceedings of the Euro-C 2014*. St. Anton Am Arlberg, pp. 451–461.

- de Dear, R., Brager, G.S., 1998. Developing an Adaptive Model of Thermal Comfort and Preference. UC Berkeley Center for the Built Environment.
- Delgarm, N., Sajadi, B., Kowsary, F., Delgarm, S., 2016. Multi-objective optimization of the building energy performance: a simulation-based approach by means of particle swarm optimization (PSO). *Appl. Energy* 170, 293–303.
- Eltaweel, A., Su, Y., 2017. Parametric design and daylighting: a literature review. *Renew. Sustain. Energy Rev.* 73, 1086–1103.
- Fajkus, M., 2013. Superficial skins? Super skins? Shading structures and thermal impact analysis. In: *Proceedings of the Advanced Building Skins - Energy Forum*. Bressanone: Advanced Building Skins, pp. 23–27.
- Ferreira, C.C., 2016. Análise de sensibilidade por meio de experimento fatorial de parâmetros de desempenho termico de envoltórias de edificações residenciais: contribuição à revisão das normas brasileiras (Unpublished doctoral dissertation). Universidade Federal de Ouro Preto, Ouro Preto, Brazil.
- Gilewski, W., Pełczyński, J., Stawarz, P., 2014. A comparative study of origami inspired folded plates. *Proc. Eng.* 91, 220–225.
- González, J., Fiorito, F., 2015. Daylight design of office buildings: optimisation of external solar shadings by using combined simulation methods. *Buildings* 2015 (5), 560–580.
- Guimarães, Í.B., 2016. Análises de incertezas e sensibilidade de arquivos climáticos e seus impactos em simulações computacionais termo energéticas (Unpublished master's thesis). Universidade Federal de Viçosa, Viçosa, Brazil.
- Hair, J.F., Anderson, R.E., Tatham, R.L., Blac, W.C., 2005. *Análise Multivariada de Dados*, fifth ed. Bookman.
- Hemmerling, M., 2010. ORIGAMICS digital folding strategies in architecture. In: *Proceedings of the 5th ASCAAD-Conference*. The Arab Society for Computer Aided Architectural Design, Fez, pp. 89–96.
- Hoff, N.J., 1966. The Perplexing Behavior of Thin Circular Cylindrical Shells in Axial Compression. Stanford University Department of Aeronautics and Astronautics.
- Hunt, G.W., Ario, I., 2005. Twist buckling and the foldable cylinder: an exercise in origami. *Int. J. Non Linear Mech.* 40, 833–843.
- Jakubiec, A., Reinhart, C.F., 2011. Diva 2.0: integrating daylight and energy simulations using Rhinoceros 3D, Daysim and EnergyPlus. In: *Proceedings of the 12th Conference of International Building Performance Simulation Association*. Sydney: International Building Performance Simulation Association, pp. 2202–2209.
- Krüger, E.L., Laroca, C., 2010. Thermal performance evaluation of a low-cost housing prototype made with plywood panels in Southern Brazil. *Appl. Energy* 87, 661–672.
- Lamberts, R., Cândido, C., de Dear, R., Vecchi, R.D., 2013. Towards a Brazilian Standard on Thermal Comfort (Research Report).
- Lebée, A., 2015. From folds to structures, a review. *Int. J. Space Struct.* 30, 55–74.
- Mardaljevic, J., Heschong, L., Lee, E., 2009. Daylight metrics and energy savings. *Light. Res. Technol.* 41, 261–283.
- Mattoccia, A., Bevilacqua, M.G., Leccese, F., Rocca, M., Rubio, R., 2016. Folded wooden responsive houses in hot arid climate. In: *Proceedings of the 7th Symposium on Simulation for Architecture and Urban Design*. Society for Modeling & Simulation International, London, pp. 231–238.
- Miura, K., 1985. *Method of Packaging and Deployment of Large Membranes in Space*, 618th ed. Institute of Space and Astronautical Sciences.
- Montgomery, D.C., Runger, G.C., Hubele, N.F., 2012. *Estatística Aplicada à Engenharia*, second ed. LTC - Livros Técnicos e Científicos, Rio de Janeiro.
- Nishiyama, Y., 2012. Miura folding: applying origami to space exploration. *Int. J. Pure Appl. Math.* 79, 269–279.
- Paoletti, I., 2006. *Building Complex Shapes: Innovation, Mass-Customization and Technology Transfer in Architecture*, first ed. Edizioni Clup, Milan.
- Peraza-Hernandez, E.A., Hartl, D.J., Malak, R.J., Lagoudas, D.C., 2014. Origami-inspired active structures: a synthesis and review. *Smart Mater. Struct.* 23, 9.
- Pereira, I.M., Assis, E.S., 2010. Avaliação de modelos de índices adaptativos para uso no projeto arquitetônico bioclimático. *Ambiente Construído* 10, 31–51.
- Pesenti, M., Masera, G., Fiorito, F., Sauchelli, M., 2015. Kinetic solar skin: a responsive folding technique. *Energy Proc.* 70, 661–672.
- Pinto, R.D.O., 2003. Avaliação pós-ocupação do desempenho térmico em edifícios de escritórios: estudo de caso utilizando análise fatorial e simulação computacional. (Unpublished master's thesis) Centro Federal de Educação Tecnológica de Minas Gerais, Belo Horizonte, Brazil.
- Reddy, T.A., 2011. *Applied Data Analysis and Modeling for Energy Engineers and Scientists*, 2011 ed. Springer Science & Business Media, Arizona.
- Reinhart, C.F., Wienold, J., 2011. The daylighting dashboard - a simulation-based design analysis for daylight spaces. *Build. Environ.* 46, 386–396.
- Roudsari, M.S., Pak, M., 2013. Ladybug: a parametric environmental plugin for grasshopper to help designers create an environmentally-conscious design. In: *Proceedings of the 13th Conference of International Building Performance Simulation Association*. Chambéry: International Building Performance Simulation Association, pp. 3129–3135.
- Sadineni, S.B., Madala, S., Boehm, R.F., 2011. Passive building energy savings: a review of building envelope components. *Renew. Sustain. Energy Rev.* 15, 3617–3631.
- Santana, L.O., Guimarães, Í.B.B., Carlo, J.C., 2015. Parametrização Aplicada ao Desempenho Energético de Edificações. *V!rus* 11.
- Tachi, T., 2010. Freeform rigid-foldable structure using bidirectionally flat-foldable planar quadrilateral mesh. In: Ceccato, C., Hesselgren, L., Pauly, M., Pottmann, H., Wallner, J. (Eds.), *Proceedings of the Advances in Architectural Geometry 2010*. Vienna, pp. 203–215.